

Gamma Radiation Shielding Characteristics of Nanocomposites Fabricated by Ultrasonic Waves-Assisted Cold Blending of Titanium Dioxide Nanoparticles and MDPE Matrix

Cachwala M. Nuago, Abdullah S. Harun*, Bakayuku Timanwabi

Faculty of Applied Sciences, Cape Peninsula University of Technology, Cape Town, REPUBLIC OF SOUTH AFRICA
Corresponding author email: abdullah2311975@yahoo.com

Abstract

In this study, hybrid nanocomposites were prepared from MDPE matrix reinforced with TiO₂ nanoparticles with different weight fractions using cold blending method assisted by ultrasonic waves. The gamma radiation shielding characteristics of these nanocomposites were introduced and compared throughout measuring parameters such as mass and linear attenuation coefficients, half-value and tenth-value thicknesses, effective atomic number, effective electron density, and effective conductivity. Different radioactive sources with different energies ranging in 0.01-16 eV were used. Results showed that adding TiO₂ nanoparticles to the MDPE matrix has reasonably enhanced the prepared nanocomposites' capability for radiation shielding as the apparent density of the samples was increased with increasing TiO₂ nanoparticles content in the composite samples. Consequently, the thickness required for shielding was reduced and attenuation parameters were increased especially at low energies where the photoelectric effect dominates. As well, samples with higher weight fractions of TiO₂ nanoparticles showed higher values of effective atomic number and effective electron density that enhances scattering and absorption efficiency. In general, the prepared hybrid nanocomposites have confirmed their effectiveness as promising materials for radiation shielding applications with good control of their characteristics according to practical requirements related to weight, cost, and mechanical performance.

Keywords: Hybrid composites; Nanocomposites; Titanium dioxide; Shielding materials

Received: November 2025; **Revised:** January 2026; **Accepted:** February 2026; **Published:** April 2026

1. Introduction

Nanocomposites are one of the most developing materials in the field of radiation shielding because they made a qualitative transformation, when compared to the conventional materials such as concrete and lead, by combining the lightweight and high efficiency in shielding against ionizing and nonionizing radiations. The performance of these materials depends on the incorporation of nanoparticles with unique physical properties in a polymer, a ceramic or a metallic matrix to produce hybrid material with ability to dissipate the radiation energy throughout mechanisms like scattering, absorption, and interference [1-3]. The heavy metal compounds such as graphene oxide, iron oxides, lead oxide and tungsten carbide are primarily used filling materials due to their high capability to react with photons and neutrons [4,5].

The most featured practical applications of nanocomposites are electrical cable shielding in the nuclear energy plants, manufacture of protective clothes for workers in medical and radiation sectors, and manufacture of spacecraft parts to protect the astronauts from cosmic radiation [6-8]. As well, nanocomposites are used in the installation of internal shielding plates in radiation imaging chambers and linear accelerators (LINACS) in hospitals. These materials are employed as a result of the quantum confinement phenomenon rising when the material dimensions are at the nanoscale and hence the active surface area is increased and the interaction with radiation is enhanced [9-11]. Furthermore, nanoparticles can be dispersed homogeneously inside a matrix in order to create tortuous paths hindering the propagation of electromagnetic waves and high-energetic particles [12]. Also, the employment of carbon nanotubes (CNTs) enhances the mechanical and thermal properties in addition to shielding characteristics. This makes the nanocomposite material capable to hold harsh conditions of temperature, pressure and radiation before rapidly deteriorate [13,14].

The manufacturing technique plays a crucial role in determining the quality if the final product as techniques like solution casting, melt extrusion, and electrodeposition are used to ensure even dispersion of the nanomaterial within the matrix medium [15,16]. However, some technical challenges

remain against the wide marketing of these materials such as high production cost of the nanoparticles, difficult control of bulk distribution and agglomeration that may lead to weakness points in the structure, in addition to the essence of understanding the interactions at the interfaces between nanofillers and matrix to guarantee the long-range stability [17,18]. Alongside, new types of hybrid nanocomposites are continuously developed to combine elements like bismuth and gadolinium to achieve wide spectrum of radiation (alpha, beta, gamma, or thermal neutrons) [19]. Recent research works showed that the incorporation of nanoparticles of large atomic numbers increases the interaction cross section with radiation, decreases both thickness required for shielding and sample total weight, which is very important in space and medical applications that require flexibility and portability. These materials are promising in the construction of small modular reactors and mobile medical facilities that needs effective shielding at reduced weight [20-23]. For environmental safety requirements, these nanocomposites are considered lower toxic than conventional lead, can be designed to be recyclable or biodegraded using eco-friendly polymers. Consequently, they contribute to achieve the sustainability standards while keeping efficient shielding [24-26]. The trend to employ the artificial intelligence (AI) in designing nanocomposites allows to predict the optimum compositions and nanostructures to shield specific radiation and hence shorten the time and reduce the cost at the production stage [27]. Finally, nanocomposites represent the future of radiation shielding industry due to their design flexibility, multifunctionality, and long-range superiority over conventional materials in performance, weight, and cost [28-30].

Medium-density polyethylene (MDPE) is a thermostat plastics that gain increasing interest in the manufacture of nanocomposites due to the unique mix of physical and chemical properties that make it optimum medium or matrix to host the nanofillers with homogeneous dispersion [31,32]. Physically, MDPE shows moderate crystallinity that prevents the accurate balance between hardness and flexibility. This facilitates the manufacturing processes such as casting and melt extrusion and therefore produces formable and tough products in the same time [33]. The relatively low density of MDPE makes it a strategic selection in the applications requiring lightweight like avionics and space in order to reduce the overall mass of the structures while attaining the required mechanical performance [34]. Chemically, MDPE shows good resistance to solvents and chemical compounds and its molecular structure based on hydrogen-rich hydrocarbon chains gives it a natural radiation shielding property via the interaction of hydrogen atoms with energetic particles like protons and neutrons and hence dissipate their energy [35].

When MDPE-based nanocomposites are prepared, various nanofillers like CNTs and graphene nano-platelets (GNPs) are incorporated within the polymer matrix. These fillers enhances the mechanical, electrical and thermal properties of the nanocomposites as the addition of small amounts of single-walled or multi-walled CNTs (SWCNTs or MWCNTs) to the MDPE can lead to drastic enhancement in the tensile strength that may reach up to 185% [36,37]. These nanocomposites are strictly tested to resist the proton irradiation to ensure stable chemical and physical properties such as wettability and surface morphology when exposed to radiation. These tests can confirm their suitability as protective materials in spacecraft and orbital planets [38,39].

Nanomaterials, and particularly titanium dioxide (TiO_2), are generally considered as the cornerstone of the modern industry of nanocomposites due to their exceptional characteristics, mainly, the huge surface-to-volume ratio, which support their reactivity and ability to affect the surrounding medium. TiO_2 nanoparticles show a special essence over other ceramic nanoparticles due to the combination of excellent performance, low cost and environmental safety [40]. TiO_2 is widely abundant material, biologically non-toxic, high chemical stability, and excellent treatability in different conditions. When the TiO_2 nanoparticles are incorporated in polymer, ceramic, or metallic matrix to produce nanocomposites, they act as fillers as well as add totally new or support existing characteristics of the produced material. Mechanically, addition of small amounts of TiO_2 nanoparticles (typically 1 wt.%) may lead to drastic enhancement in the mechanical properties of the polymer matrix up to 100% due to the huge surface area allowing strong interactions with the polymeric chains that increases hardness, toughness and stress resistance [41]. As well, the ability of TiO_2 nanoparticles to absorb and reflect UV radiation enhances the aging resistance of the nanocomposites and hence their performance at elevated temperatures. This makes them optimum material for protective coatings in the harsh industrial environments [42].

In this work, TiO_2 nanoparticles with different weight fractions were incorporated in MDPE matrix to produce hybrid nanocomposites and the shielding characteristics against gamma radiation were determined and compared.

2. Experimental Work

The nanocomposite material was prepared by the cold blending method by mixing different weight fractions of TiO₂ nanopowder as filler with MDPE powder as matrix. This method was assisted by the ultrasonic waves in order to produce structurally homogeneous samples. The apparent density was measured in g/cm³ as an indicator for dispersion quality. The weighed powders were placed in clean and dry glass beaker as the toluene was added to dissolve the polymer (MDPE) and form a suspension with the nanoparticles. The beaker is sealed to prevent the evaporation of the solvent and placed in the ultrasonic bath operated at 40 kHz for 30-60 minutes. The ultrasonic waves generate an acoustic cavitation to blow up the tiny bubbles within the liquid and hence produce high energy to disassemble the agglomerates of the nanoparticles and disperse them evenly in the polymer solution. This would ensure the maximum structural homogeneity before pouring the suspension in the molds. This homogeneity can attain the apparent density, which was increased with increasing the weight fraction of the TiO₂ nanopowder as shown in table (1). This increase may be smaller at higher weight fractions of the nanopowder due to the possible microporosity or localized agglomerations within the nanocomposite sample. Figure (1) explains schematically the experimental part of this work.

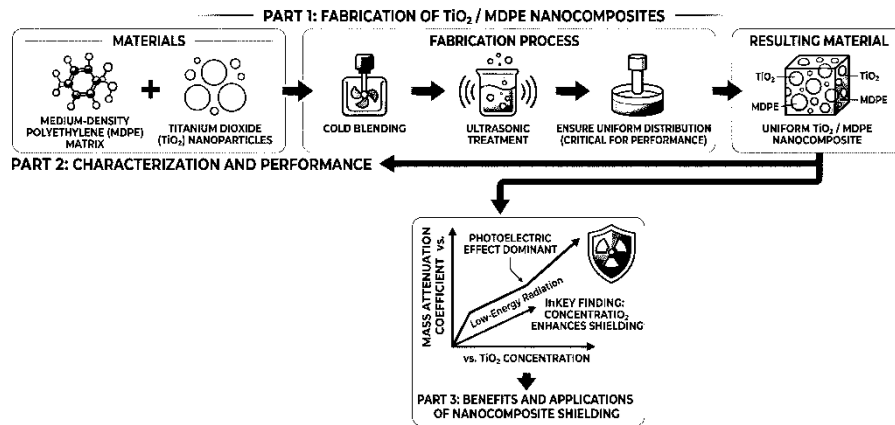


Fig. (1) Flow chart explaining the experimental part of this work

After the step of ultrasonic bath is completed, the suspensions were poured in silicon molds as discs with diameter of 5cm. These samples were left at room temperature for 24 hours to solidify as a result of the slow evaporation of the solvent to avoid the formation of bubbles and surface cracks. The samples were then dried in a vacuum oven at low temperature (40-50 °C) to remove any residual solvent and ensure stable dimensions. The apparent density was firstly measured for all samples. This cold blending method assisted by the ultrasonic waves is effective, simple, and low cost and can be developed by using green solvents instead of toluene.

The radiation shielding characteristics were determined by measuring the shielding parameters such as mass attenuation coefficient (MAC), linear attenuation coefficient (LAC), half-value length (HVL), tenth-value length (TVL), mean free path (MFP), effective atomic number (Z_{eff}), effective electron density (N_{eff}), and effective conductivity (C_{eff}) as functions of incident energy of gamma photons. These photon were obtained by three different radioactive sources (Cs-137, I-131, and Na-22) with eight different energies (0.2835 and 0.6617 eV for Cs-137, 0.284, 0.3645, 0.637, and 0.723 eV for I-131, and 0.511 and 1.275 eV for Na-22). The parameters mentioned above were determined by the following equations respectively [28]:

$$MAC = \frac{\mu}{\rho} = \frac{1}{\rho x} \ln \left(\frac{I_0}{I} \right) \quad (1)$$

$$LAC = \mu = \frac{1}{x} \ln \left(\frac{I_0}{I} \right) \quad (2)$$

$$HVL = \frac{\ln 2}{\mu} \quad (3)$$

$$TVL = \frac{\ln 10}{\mu} \quad (4)$$

$$MFP = \frac{1}{\mu} \quad (5)$$

$$Z_{eff} = \frac{\sigma_a}{\sigma_e} = \frac{\sum f_i A_i \left(\frac{\mu}{\rho}\right)_i}{\sum f_j \frac{A_j}{Z_j} \left(\frac{\mu}{\rho}\right)_j} \quad (6)$$

$$N_{eff} = \frac{N_A Z_{eff}}{\sum f_i A_i} \quad (7)$$

$$C_{eff} = 10^3 \left(\frac{N_{eff} \rho e^2 \tau}{m_e} \right) \quad (8)$$

where I and I_0 are the transmitted and incident radiation intensities, respectively, x is the sample thickness, μ is the linear absorption coefficient, ρ is the density of material, σ_a and σ_e are the atomic and electronic cross sections, respectively, f_i is the ratio of number of atoms of an individual element, A_i refers the atomic weight of each specific element present in the target material, e is the electron charge, m is the electron mass, τ is the relaxation time

Table (1) Composition and density of the nanocomposite samples fabricated in this work

Sample	MDPE (wt.%)	TiO ₂ NPs (wt.%)	Apparent Density (g/cm ³)
1	100	0	0.9400
2	95	5	0.9771
3	90	10	1.017
4	85	15	1.061
5	80	20	1.108
6	75	25	1.160
7	70	30	1.217
8	65	35	1.280
9	60	40	1.350
10	55	45	1.428
11	50	50	1.515



Fig. (1) A photograph of nanocomposite samples fabricated in this work

3. Results and Discussion

Figure (2) shows the variation of MAC with incident photon energy for the prepared samples. For all samples, the MAC apparently decreases with incident energy and this behavior completely agrees with the physical mechanisms of the radiation-matter interaction. At low energies (<0.1 eV) shown in Fig. (2b), the values of MAC are relatively high as the photoelectric effect is the dominant mechanism, which depends on the total absorption of photons and is directly proportional to the high atomic number of titanium in TiO₂ filler. At the medium energies (0.1-1 eV) shown in Fig. (2c), a gradual decrease in the MAC values is observed as the Compton scattering is the dominant mechanism, which depends on the electron density in the sample. Here, the role of the hydrogen-rich MDPE matrix in enhancing the scattering appears as the pair production is theoretically possible but limited due to the energies used. Very slight differences are observed in the MAC values for all samples and – at energies lower than 0.1533 eV – the MAC values increase with increasing weight fraction of TiO₂ nanoparticles, whereas they decrease with increasing weight fraction of TiO₂ nanoparticles at energies higher than 0.1533 eV. This may assign an inversion point at this energy. At the high energies (>1 eV) shown in Fig. (2d), the last behavior of MAC values with weight fraction of TiO₂ nanoparticles continues until 6 eV as a constant value for all samples is observed, beyond which, a behavior identical to that at energies lower than 0.1533 eV is seen. These data presents a quantitative evidence for the successful fabrication of

TiO₂/MDPE nanocomposites as promising materials in radiation shielding applications. The optimum content of TiO₂ nanoparticles can be selected depending on the radiation energy to be shielded with balanced cost, weight and mechanical characteristics required for the final application.

Figure (3) shows the variation of LAC with incident photon energy for the prepared samples. The behavior of LAC is similar to that of MAC with photon energy but with more differences and no inversion points were observed. Accordingly, the samples with higher weight fraction of TiO₂ nanoparticles show higher values of LAC while their corresponding MAC values are very identical. The higher density means that larger number of atoms per unit volume exist and hence better opportunities to interact with incident radiation.

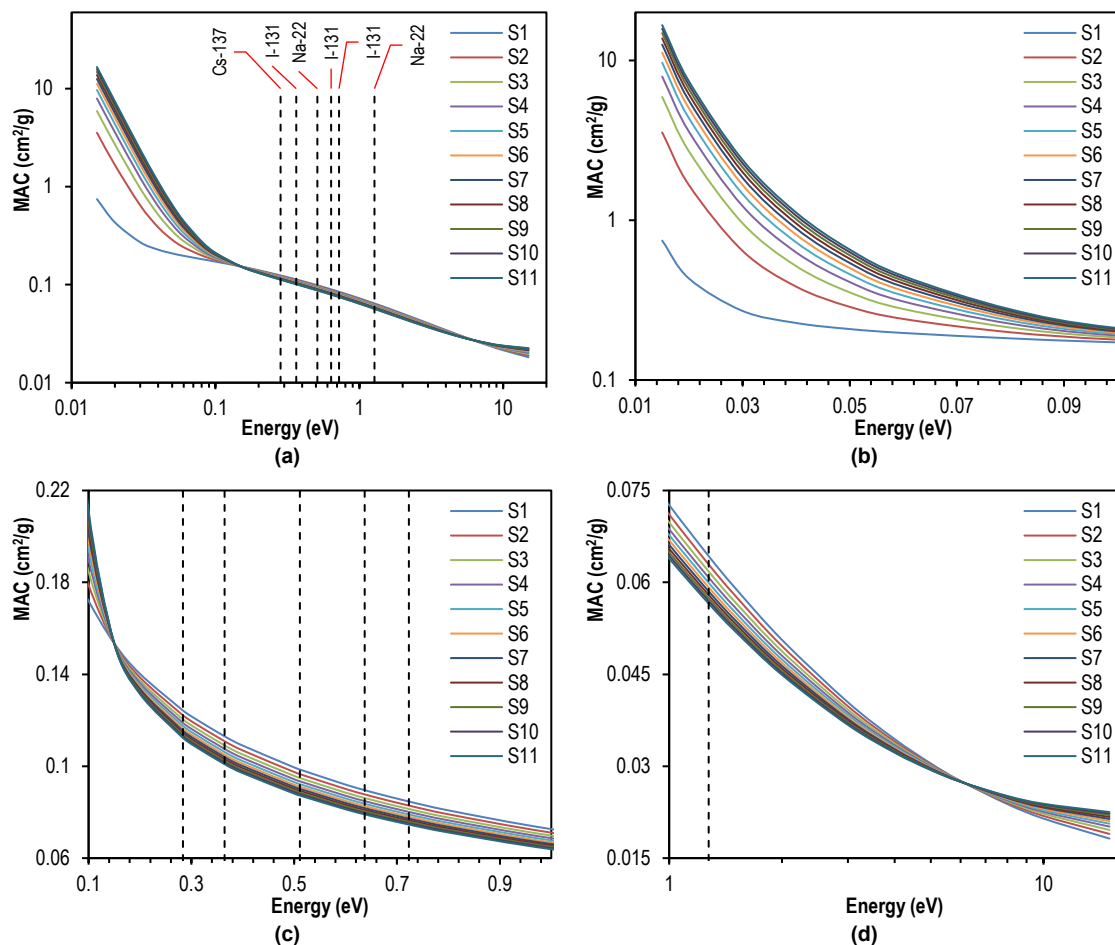


Fig. (2) Variation of MAC with incident gamma photon energy for the prepared samples within (a) 0.01-16 eV, (b) 0.01-0.1 eV, (c) 0.1-1 eV, and (d) 1-16 eV

Figure (4) shows the variation of HVL with incident photon energy for the prepared samples. As the HVL represents the thickness required to reduce the radiation intensity to half its value, so, the shielding is enhanced as the HVL value is decreased. Adding TiO₂ nanoparticles to the MDPE matrix lead to decrease the thickness required for shielding, decrease the corresponding HVL values, and hence decrease the sample weight and cost. This is compatible with the fundamental concept of using nanocomposites for shielding applications with apparent role of large atomic number of titanium ($Z=22$) in TiO₂ nanoparticles as it shows much more efficient photon absorption when compared to carbon and hydrogen in the MDPE structure, especially at low energies where the photoelectric effect dominates as an approximate proportionality to Z^4 . At moderate and high energies, the samples show comparable values of HVL.

Since TVL is defined as the sample thickness required to reduce the transmitted intensity to tenth (10%) its value, its behavior with photon energy is expected to be very similar to that of HVL, as shown in Fig. (5). As well, the mean free path (MFP) represents the reciprocal of linear attenuation coefficient

(LAC, μ), so, its variation with photon energy is similar to those of HVL and TVL with photon energy. It is conceptual that increasing the content of TiO₂ nanoparticles in the nanocomposite samples results in corresponding increase in the material density and hence decrease the spaces between particles, i.e., decrease the distance traversed by incident/scattered photons before scattered again.

In composite materials consisting of more than one element, the effective atomic number (Z_{eff}) must be considered to introduce the shielding characteristics rather than atomic number. Higher values of Z_{eff} lead to better shielding performance of the nanocomposite material and the Z_{eff} value is increased as the content of the metallic element (Ti) in the ceramic (TiO₂) is increased. Figure (7) shows the variation of effective atomic number (Z_{eff}) with incident gamma photon energy for the prepared samples within 0.01-16 eV. The differences between samples are much more apparent than differences seen in MAC, LAC, HVL, TVL and MFP due to the large differences between atomic and electronic cross sections.

With direct proportionality of the effective electron density (N_{eff}) with the effective atomic number (Z_{eff}), it is expected that the variation of N_{eff} with incident photon energy be identical to that of Z_{eff} with incident photon energy. However, differences between samples can be seen at low energies whereas they get smaller at higher energies (>0.1 eV) with systematic behavior with increasing the weight fraction of TiO₂ nanoparticles in the composite samples, as shown in Fig. (8).

As can be seen in Fig. (9), the behavior of conductivity of the prepared samples as a function of incident photon energy is much more uniform than that of Z_{eff} and N_{eff} . This can be attributed to the insertion of additional constants, such as electron charge, electron mass, material density and relaxation time. The enhancement of conductivity due to the addition of TiO₂ nanoparticles to the MDPE matrix is apparent at low energies (<0.1 eV) and weaker at higher energies (>0.1 eV).

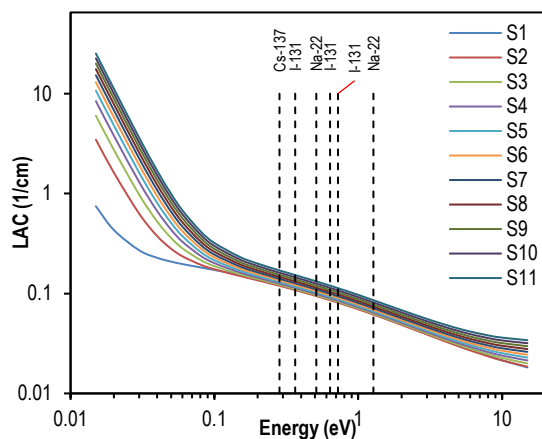


Fig. (3) Variation of LAC with incident gamma photon energy for the prepared samples within 0.01-16 eV

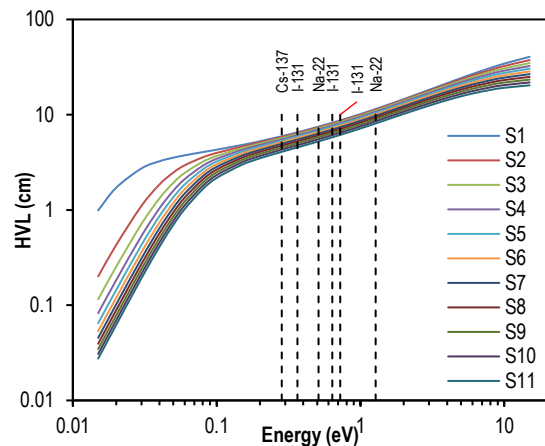


Fig. (4) Variation of HVL with incident gamma photon energy for the prepared samples within 0.01-16 eV

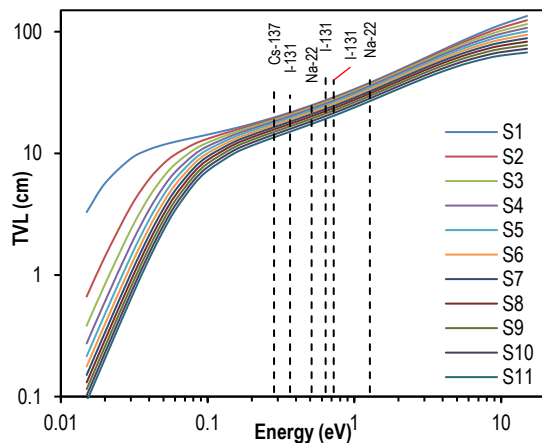


Fig. (5) Variation of TVL with incident gamma photon energy for the prepared samples within 0.01-16 eV

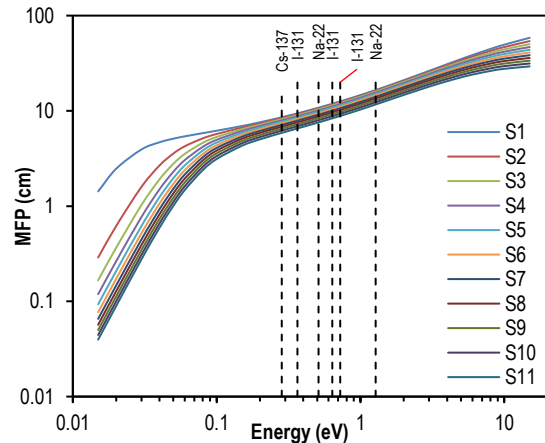


Fig. (6) Variation of MFP with incident gamma photon energy for the prepared samples within 0.01-16 eV

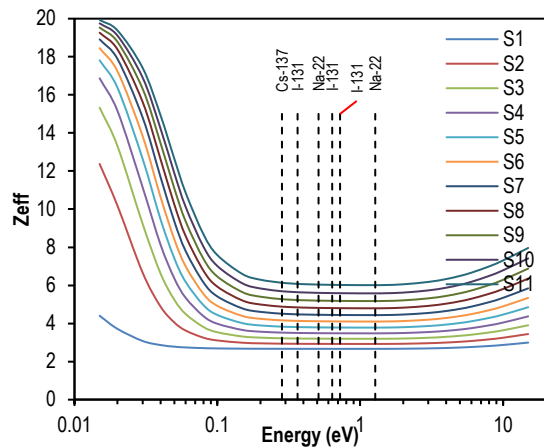


Fig. (7) Variation of effective atomic number (Z_{eff}) with incident gamma photon energy for the prepared samples within 0.01-16 eV

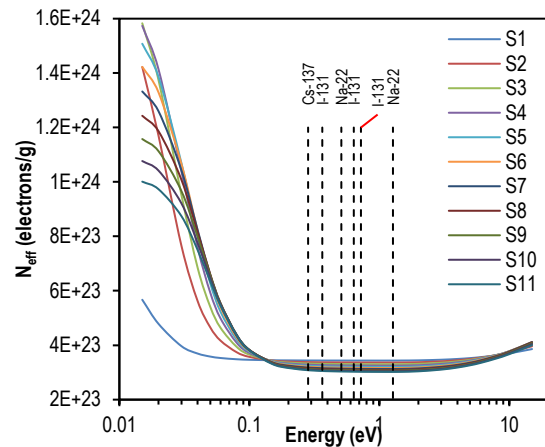


Fig. (8) Variation of effective electron density (N_{eff}) with incident gamma photon energy for the prepared samples within 0.01-16 eV

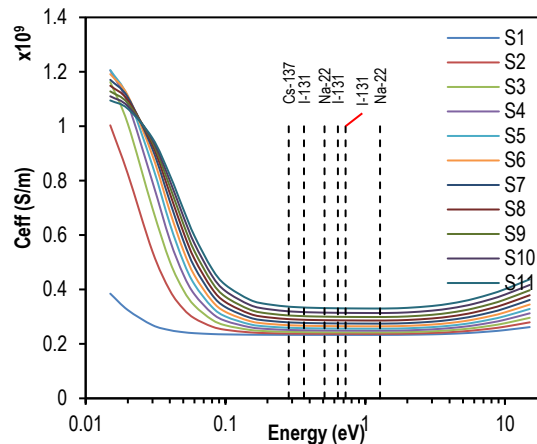


Fig. (9) Variation of effective conductivity (C_{eff}) with incident gamma photon energy for the prepared samples within 0.01-16 eV

4. Conclusion

In concluding remarks, the addition of TiO_2 nanoparticles to the MDPE matrix reasonably enhances the characteristics of MDPE/ TiO_2 nanocomposites for gamma radiation shielding as the apparent density is increased and shielding parameters are decreased with increasing weight fraction of TiO_2 nanoparticles in the composite samples particularly at low energies where the photoelectric effect dominates. The behaviors of mass and linear attenuation parameters agree with the physical mechanisms of radiation-matter interaction, which confirms the successful preparation. In general, the prepared hybrid nanocomposites are promising materials for radiation shielding applications due to their lightweight and high efficiencies.

References

- [1] M.I. Abbas et al., "Investigation of Gamma-Ray Shielding Properties of Bismuth Oxide Nanoparticles with a Bentonite-Gypsum Matrix", *MDPI Mater.*, 16 (2023) 2056.
- [2] A.H. Abdalsalam et al., "Investigation of gamma ray attenuation features of bismuth oxide nano powder reinforced high-density polyethylene matrix composites", *Radiat. Phys. Chem.*, 168 (2020) 108537.
- [3] A. Acevedo-Del-Castillo et al., "A Brief Review on the High-Energy Electromagnetic Radiation-Shielding Materials Based on Polymer Nanocomposites", *Int. J. Mol. Sci.*, 22 (2021) 9079.
- [4] M.T. Alabsy et al., "Enhancing the Gamma-Radiation-Shielding Properties of Gypsum-Lime-Waste Marble Mortars by Incorporating Micro and Nano-PbO Particles", *MDPI Mater.*, 16 (2023) 1577.
- [5] I.G. Alhindawy et al., "Optimizing gamma radiation shielding with cobalt-titania hybrid nanomaterials", *Sci. Rep.*, 13 (2023) 8936.
- [6] A.H. Almuqrin, M. Elsafi and M.I. Sayyed, "Radiation shielding characteristics of PbO-BaO-B₂O₃-ZnO glass system against gamma rays: experimental study", *Opt. Quant. Electron.*, 56 (2024) 1121.
- [7] A.H. Alsaab and S. Zeghib, "Study of Prepared Lead-Free Polymer Nanocomposites for X- and Gamma-ray Shielding in

- Healthcare Applications”, *Polymers*, 15 (2023) 2142.
- [8] G. Angarita et al., “Synthesis of alumina thin films using reactive magnetron sputtering method”, *IOP Conf. Ser.: J. Phys.*, 850 (2017) 012022.
- [9] S. Ayub et al., “Preparation Methods for Graphene Metal and Polymer Based Composites for EMI Shielding Materials: State of the Art Review of the Conventional and Machine Learning Methods”, *MDPI Metals*, 11 (2021) 1164.
- [10] R. Darwesh et al., “Improved radiation shielding properties of epoxy resin composites using Sb_2O_3 and Al_2O_3 nanoparticles additives”, *Annals Nucl. Ener.*, 200 (2024) 110385.
- [11] A.M. El-Khatib et al., “Gamma Attenuation Coefficients of Nano Cadmium Oxide/High density Polyethylene Composites”, *Sci. Rep.*, 9 (2019) 16012.
- [12] M. Elsafi et al., “Grafting red clay with Bi_2O_3 nanoparticles into epoxy resin for gamma-ray shielding applications”, *Sci. Rep.*, 13 (2023) 5472.
- [13] S. Geetha et al., “EMI Shielding: Methods and Materials - A Review”, *J. Appl. Polym. Sci.*, 112 (2009) 2073-2086.
- [14] M.H. Ghozza, “Radiation Attenuation Properties of BaMnO_3 Doping Nickel Semiconductor Perovskite Using Phys-X/PSD Software”, *Arab. J. Nucl. Sci. Appl.*, 56(3) (2023) 27-40.
- [15] M.M. Gouda et al., “Comparative study between micro- and nano-carbon with epoxy for gamma shielding applications”, *Carbon Lett.*, 34 (2024) 1129-1141.
- [16] A.K. Gupta et al., “Study of electromagnetic shielding effectiveness of metal oxide polymer composite in their bulk and layered forms”, *Enviro. Sci. Pollut. Res.*, 28 (2021) 3880-3887.
- [17] O.A. Hammadi, “Production of nanopowders from physical vapor deposited films on nonmetallic substrates by conjunctional freezing-assisted ultrasonic extraction method”, *Proc. IMechE, Part N, J. Nanomater. Nanoeng. Nanosyst.*, 232(4) (2018) 135-140.
- [18] M.Y. Hanfi et al., “Influence of ZnO variation on glass characteristics: Physical, mechanical properties, and radiation shielding”, *Ceram. Int.*, 50 (2024) 53073-53082.
- [19] M.D. Hassib et al., “Boro-silicate glasses co-doped $\text{Er}^{3+}/\text{Yb}^{3+}$ for optical amplifier and gamma radiation shielding applications”, *Physica B: Cond. Matter.*, 567 (2019) 37-44.
- [20] R. Jalali et al., “Recent progress and perspective in additive manufacturing of EMI shielding functional polymer nanocomposites”, *Nano Res.*, 16(1) (2023) 1-17.
- [21] D. Jiang et al., “Electromagnetic Interference Shielding Polymers and Nanocomposites - A Review”, *Polym. Rev.*, 59(2) (2019) 280-337.
- [22] S. Joshia et al., “Epoxy-based Light Weight Gamma Ray Shielding Materials”, *Indian J. Pure Appl. Phys.*, 60 (2022) 274-282.
- [23] S.I. Jubair and A.H. Al-Mashhadani, “Shielding properties and buildup factor of $\text{Al}_2\text{O}_3/\text{PbO}$ -based ceramic materials”, *Nucl. Instrum. Meth. Phys. Res. B*, 529 (2022) 7-11.
- [24] N.A. Kawady et al., “Fabrication, characterization, and gamma ray shielding properties of PVA-based polymer nanocomposite”, *J. Mater. Sci.*, 57 (2022) 11046-11061.
- [25] M. Krzystyniak et al., “Nanocomposite materials as observed by mass-selective neutron Spectroscopy”, *J. Phys. Commun.*, 8 (2024) 022001.
- [26] C. Liang et al., “Structural Design Strategies of Polymer Matrix Composites for Electromagnetic Interference Shielding: A Review”, *Nano-Micro Lett.*, 13 (2021) 181.
- [27] S. Maity and A. Chatterjee, “Conductive polymer-based electro-conductive textile composites for electromagnetic interference shielding: A review”, *J. Indust. Textiles*, 47(8) (2018) 2228-2252.
- [28] J. Martin, “**Physics of Radiation Protection**”, 2nd ed., Wiley-VCH Verlag GmbH (Weinheim, 2006), p. 8, 605, 699.
- [29] R. Moučka, S. Goňa and M. Sedláčik, “Accurate Measurement of the True Plane-Wave Shielding Effectiveness of Thick Polymer Composite Materials via Rectangular Waveguides”, *MDPI Polym.*, 11 (2019) 1603.
- [30] M. Nadeem et al., “Development of Electromagnetic Interference shielding materials over time: A review”, *Int. J. Nanoelectron. Mater.*, 14(1) (2021) 71-98.
- [31] L. Omana et al., “Recent Advances in Polymer Nanocomposites for Electromagnetic Interference Shielding: A Review”, *ACS Omega*, 7 (2022) 25921-25947.
- [32] A.R. Pai et al., “Recent Progress in Electromagnetic Interference Shielding Performance of Porous Polymer Nanocomposites - A Review”, *Energies*, 15 (2022) 3901.
- [33] P.M.V Raja and A.R. Barron, “Physical Methods in Chemistry and Nano Science”, Rice University, LiberTexts (2024), p. 59.
- [34] S. Raja, G. Koperundevi and M. Eswaran, “Effect of Microwave Irradiation on the Dielectric Characteristics of Semi-Conductive Nanoparticle-Based Nanofluids: Progress towards the Microwave Synthesis”, *Micromachines*, 14 (2023) 1194.
- [35] E. Rajasekhar et al., “Mass Attenuation Coefficient Measurements of Some Nanocarbon Allotropes: A New Hope for Better Low Cost Less-Cumbersome Radiation Shielding Over A Wide Energy Range”, *J. Nucl. Phys. Mater. Sci. Rad. Appl.*, 5(2) (2018) 311-317.
- [36] Y.S. Rammah et al., “Gamma ray exposure buildup factor and shielding features for some binary alloys using MCNP-5 simulation code”, *Nucl. Eng. Technol.*, 53(8) (2021) 2661-2668.
- [37] K. Sathish Kumar et al., “Polymeric materials for electromagnetic shielding - A review”, *Mater. Today: Proceed.*, 47(15) (2021) 4925-4928.
- [38] M.I. Sayyed et al., “Experimental investigation of structural and radiation shielding features of $\text{Li}_2\text{O}-\text{BaO}-\text{ZnO}-\text{B}_2\text{O}_3-\text{Bi}_2\text{O}_3$ glass systems”, *Radiat. Phys. Chem.*, 218 (2024) 111640.
- [39] M.I. Sayyed et al., “ $\text{Bi}_2\text{O}_3-\text{B}_2\text{O}_3-\text{ZnO}-\text{BaO}-\text{Li}_2\text{O}$ glass system for gamma ray shielding applications”, *Optik*, 201 (2020) 163525.
- [40] K. Shahapurkar et al., “Comprehensive review on polymer composites as electromagnetic interference shielding materials”, *Polym. Polym. Compos.*, 30 (2022) 1-17.
- [41] F. Shivanand, M. Eljeeva and E. Somveer, “Synthesis and characterization of aluminum oxide nanoparticles”, *The Pharma Innov. J.*, 11(6) (2022) 1068-1072.
- [42] K.J. Singh, S. Kaur and R.S. Kaundal, “Comparative study of gamma ray shielding and some properties of $\text{PbO}-\text{SiO}_2-\text{Al}_2\text{O}_3$ and $\text{Bi}_2\text{O}_3-\text{SiO}_2-\text{Al}_2\text{O}_3$ glass systems”, *Radiat. Phys. Chem.*, 96 (2014) 153-157.